4ème Conférence Internationale des Energies Renouvelables (CIER-2016)
Proceedings of Engineering and Technology – PET
Vol.17, pp.21 - 27

Thermal interaction effect between two different Phase Change Materials encapsulated in spheres in a water flow.

RACHEDI Khouiled[#1], KORTI Abdel Illah Nabil [#2], RETERI Ahmed[#3]

[#] *ETAP laboratory, Department of Mechanical Engineering, University of tlemcen, B. P. 230, Tlemcen 13000, Algérie.*

[1]rkhouiled@gmail.com

[2]korti72@yahoo.fr

[3]reteriahmed@hotmail.com

***Abstract*—The present work is for objective to carry out a computational study on the thermal behavior of two different phase change materials (PCMs), inside spherical nodules, in both charging and discharging modes. Water is used as the heat transfer fluid (HTF). The thermal and dynamical behavior of both PCMs, i.e. PCM1 and PCM2, filled in two capsules, is detailed at the beginning of this study. The results indicate that for the height velocity of water flow, the latent heat energy packed by two different PCMs without thermal interaction is the arithmetical addition between them. Whereas, from v = 10^{-5}, the thermal interaction between two different PCMs cannot be neglected, and the energy stored is not the arithmetic addition. The thermal interaction appears clearly in the discharging mode. Thus, the thermal interaction has accelerated the discharging of PCM2. Whereas, the discharging of PCM1 is prolonged by this thermal interaction.**

Keywords —* Different phase change materials, Thermal behaviour, spherical nodules, thermal interaction.

I. INTRODUCTION

Several studies are carried out on phase change materials over the last three decades. Phase change materials are very interesting due to their absorbing of large amount of energy as latent heat at a constant phase transition temperature. Following the literature review according to Telkes and Raymond [1], the first study of phase change materials was carried out in the 1940s. There are few work reported until the 1970s. After that, the first study on PCM was presented by Barkmann and Wessling [2] for use in buildings, and later by other researchers [3-4]. Sokolov and Keizman [5] presented the applications of PCM in a solar collector for first time at 1991, and later by others,e.g. Rabin et al. [6], Enibe [7,8], and Tey et al. [9]. Also, there are a few review papers on energy thermal storage and phase change material [10,11]. Following them, a beneficial review of thermal energy storage based on PCM was presented by Zalba et al. [12]. They classified types of PCM based on material properties, heat transfer and its applications. Modelling the thermal behaviour of latent heat thermal energy storage is complex [13]. There are problems associated to the nonlinear motion of the solid–liquid interface, the possible presence of buoyancy driven flows in the melt, the conjugate heat transfer between the encapsulated phase change material and the heat transfer fluid in the storage tank and the volume expansion of the PCM upon melting–solidification.

Korti [14], developed a transient two-dimensional (2D) mathematical model for double-pass solar collector with phase change material (PCM) spheres media in the lower channel. Two different types were studied in various configurations, parallels and series. The results show that the presence of the PCM spheres at the bottom of the absorber is the best configuration and allows increasing the outlet temperature. Also, with combining several types of PCM we can improve significantly the thermal performance of collector.

In the present work, we will proved that the thermal interaction between two different PCMs cannot be neglected where the heat transfer fluid is too small, and the energy stored is not the arithmetic addition between them. All results will be present later in this paper.

II. PHYSICAL MODEL

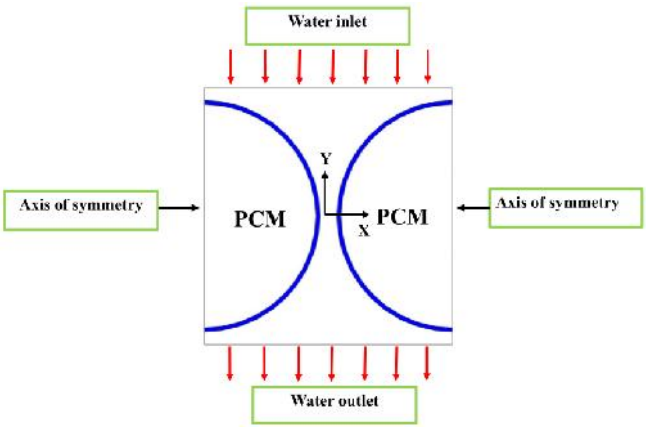

Fig. 1 Computational domains: Two spheres filled with PCMs placed horizontally.

ISSN 2356-5608

Fig.1 shows the computational domains. The aluminum spherical nodules are with 55 mm in outer diameter, 1mm in thickness, with 4 mm spacing between the two spheres and the domain boundaries. A heat transfer fluid (liquid water) flows around the spheres containing the phase change materials. During the charge mode, the simulation domain is maintained at a lower temperature than the initial melting temperature of the PCMs. The end of total melting of PCMs is the beginning of the discharge mode. The inlet temperature of water and its velocity are maintained uniforms in both charging and discharging modes.
The problem was studied in three different cases:

- Case 1 represents the behavior of the two spheres filled with PCM1, and case 2 when they are filled with PCM2.
- Case 3 represents the behavior of the two spheres filled with different PCMs; i.e. PCM 1 and PCM2.

The thermo-physical properties of the PCMs used in this study are presented in table1.

Table 1 Thermo-physical characters of PCM [15].

	PCM1	PCM2
Density (Solid), [kg. m^{-3}]	844	848
Density (liquid), [kg. m^{-3}]	760	767
Specific heat(Solid), [$J.kg^{-1} K^{-1}$]	2052	1650
Specific heat(liquid), [$J.kg^{-1} K^{-1}$]	2411	1863
Thermal conductivity (Solid), [$W.m^{-1}.K^{-1}$]	0.4	0.4
Thermal conductivity (liquid), [$W.m^{-1}.K^{-1}$]	0.15	0.15
Viscosity (liquid), [Pa.s]	4.9×10^{-3}	5.6×10^{-3}
Expansion coefficient (liquid), [K^{-1}]	8.3×10^{-4}	7.7×10^{-4}
Melting temperature, [°C]	42–44	50-52
Heat of fusion, [$J.kg^{-1}$]	1.68×10^{5}	2×10^{5}

III. MATHEMATICAL MODEL

A. Water:

Continuity equation:

$$\frac{\partial u_w}{\partial x}+\frac{\partial v_w}{\partial y}=0 \qquad (1)$$

x-direction momentum equation

$$\rho_w\left(\frac{\partial u_w}{\partial t}+u_w\frac{\partial u_w}{\partial x}+v_w\frac{\partial u_w}{\partial y}\right)=\mu_w\left(\frac{\partial^2 u_w}{\partial x^2}+\frac{\partial^2 u_w}{\partial y^2}\right)-\frac{\partial P}{\partial x} \qquad (2)$$

y-direction momentum equation:

$$\rho_w\left(\frac{\partial v_w}{\partial t}+u_w\frac{\partial v_w}{\partial x}+v_w\frac{\partial v_w}{\partial y}\right)=\mu_w\left(\frac{\partial^2 v_w}{\partial x^2}+\frac{\partial^2 v_w}{\partial y^2}\right)-\frac{\partial P}{\partial y} \qquad (3)$$

Thermal energy equation:

$$\rho_w c_w\left(\frac{\partial T_w}{\partial t}+u_w\frac{\partial T_w}{\partial x}+v_w\frac{\partial T_w}{\partial y}\right)=\alpha_w\left(\frac{\partial^2 T_w}{\partial x^2}+\frac{\partial^2 T_w}{\partial y^2}\right) \qquad (4)$$

Were (u_p, v_p) are components of velocity vector of water, ρ_w is the water density, μ_w is its dynamic viscosity, c_w is its heat capacity, α_w is its effective thermal conductivity, P the pressure and g the gravitational acceleration.

B. Aluminum spheres:

Only the thermal energy equation governs the aluminum thickness of sphere.

$$\frac{\partial(\rho_{Al}\, c_{Al} T_{Al})}{\partial t}=\alpha_{Al}\left(\frac{\partial^2 T_{Al}}{\partial x^2}+\frac{\partial^2 T_{Al}}{\partial y^2}\right) \qquad (5)$$

C. PCMs:

PCMs are described by the continuity equation, the equation of motion modified in the x and y directions, and the thermal energy equation.

Continuity:

$$\frac{\partial u_p}{\partial x}+\frac{\partial v_p}{\partial y}=0 \qquad (6)$$

Modified *x*-direction momentum:

$$\rho_p\left(\frac{\partial u_p}{\partial t}+u_p\frac{\partial u_p}{\partial x}+v_p\frac{\partial u_p}{\partial y}\right)=\mu_p\left(\frac{\partial^2 u_p}{\partial x^2}+\frac{\partial^2 u_p}{\partial y^2}\right)-\frac{\partial P}{\partial x}+S_x \qquad (7)$$

Modified y-direction momentum:

$$\rho_p\left(\frac{\partial v_p}{\partial t}+u_p\frac{\partial v_p}{\partial x}+v_p\frac{\partial v_p}{\partial y}\right)=\mu_p\left(\frac{\partial^2 v_p}{\partial x^2}+\frac{\partial^2 v_p}{\partial y^2}\right)-\frac{\partial P}{\partial y}+\rho_p g\ \beta_p\left(T_p-T_{ref\ p}\right)+S_y \qquad (8)$$

The source terms S_x and S_y allow modifying the momentum equations in the mushy zone and in the solid phase. They are expressed according to Darcy's law as follows [16]:

$$S_x=Au_p;\ S_y=Av_p \qquad (9)$$

ISSN 2356-5608

$$A = C\frac{(1-f_\ell)^2}{f_\ell^{\,3}+b} \tag{10}$$

The liquid fraction, described by a linear function, ranges from zero in the solid phase to one in the liquid phase,

$$f_\ell = \begin{cases} 1 & \text{if } T > T_\ell \\ \dfrac{T-T_s}{T_\ell - T_s} & \text{if } T_s < T < T \\ 0 & \text{if } T < T_S \end{cases} \tag{11}$$

Where A is the porosity function, C is a mushy zone constant which is fixed ($C = 10^5$ kg/m^{3}s) for the present study [17]. In the liquid phase ($f_l = 1$), the porosity function and thus the Darcy-type source term turns to zero. When approaching the solid phase, the liquid fraction turns to zero. To avoid the division by zero in the solid phase, a small numerical constant b is introduced.

Modified thermal energy equation:

$$\rho_p\left(\frac{\partial H}{\partial t} + u_p\frac{\partial H}{\partial x} + v_p\frac{\partial H}{\partial y}\right) = \alpha_p\left(\frac{\partial^2 T_p}{\partial x^2} + \frac{\partial^2 T_p}{\partial y^2}\right) \tag{12}$$

To describe the enthalpy in Eq. (12), the specific sensible enthalpy h is extended by the latent heat of fusion L as a function of temperature:

$$H = h + L(T) = \int_{T_{ref}}^{T_p} c_p\, dT + f_\ell L \tag{13}$$

Applying (13) to (12) leads to the common energy conservation equation for phase change processes:

$$\rho_p c_p\left(\frac{\partial T_p}{\partial t} + u_p\frac{\partial T_p}{\partial x} + v_p\frac{\partial T_p}{\partial y}\right) = \alpha_p\left(\frac{\partial^2 T_p}{\partial x^2} + \frac{\partial^2 T_p}{\partial y^2}\right) + S_h \tag{14}$$

$$S_h = -\rho_p L\left(\frac{\partial f_\ell}{\partial t} + u_p\frac{\partial f_\ell}{\partial x} + v_p\frac{\partial f_\ell}{\partial y}\right) \tag{15}$$

Were (u_p, v_p) are components of velocity vector of the liquid PCM, ρ_p is the density of the PCM, μ_p is dynamic viscosity, β_p is thermal expansion coefficient, c_p is its heat capacity, and α_p is its effective thermal conductivity, $T_{ref,p}$ is reference temperature of PCM, it was set equal to that of inlet temperature of hot water.

IV. Boundary and Initial conditions

At the initial time ($t = 0$) of the charging mode, the whole computational domain is maintained at a constant temperature, below the melting temperature of the PCMs ($T_0 = 32\ ^0$C). The end of the charging mode is the beginning of the discharging one. Moreover, the no-slip boundary condition is applied to the walls of the sphere. The right and left boundaries are adiabatic, whereas the upper one is the inlet flow boundary, with a height velocity of 0.3 m/s to reduce the interaction between two adjacent spheres, and uniform temperatures of 70 °C and 32 °C for charging and discharging modes, respectively. The lower wall is the outflow boundary and the heat flux continuity at the wall of spheres.

V. Results and discussions

Three different velocity of water flow (10^{-4}, 10^{-5} and 10^{-6} m/s) were tested to analyse the effect of water velocity on the thermal interaction between two adjacent spheres filed with different PCMs. At t = 4000 *s*, the discharging mode starts for all three velocities. Figs. 2 and 3 show the water velocity effect during the charging and discharging phases at 2000 and 6000 s, respectively. During the charging mode for an inlet velocity of 10^{-4} m/s, it can be seen that the liquid fraction and the thermal behavior of PCM 1 in case 1 is identical to PCM1 in case 3. In addition, the liquid fraction and the thermal behavior of PCM 2 in Case 2 is identical to PCM2 in Case 3. Thus, there is no visible thermal interaction between the two adjacent PCMs. As presented in (table 2), the liquid fraction at this stage is about 0.87 and 0.54 for PCM1 and PCM2, respectively. During the discharging mode, the thermal interaction remains no visible for an inlet velocity of 10^{-4} m/s. The two PCMs in Case 3 have the same liquid fraction of that of cases 1 and 2. It equals 0.57 and 0.39 for PCM1 and PCM2, respectively. Therefore, we can say that without thermal interaction, the latent heat energy stored by two different PCMs (Case 3) is the arithmetical addition of that stored with the same PCM in cases (1) and (2). During the charging mode, the latent heat energy stored is 2.9132×10^5, 2.16×10^5 and 2.5416×10^5 kJ/kg in cases (1), (2) and (3), respectively. During the discharging mode, these values become 1.9152×10^5, 1.56×10^5 and 1.7376×10^5 kJ/kg.

For an inlet velocity of 10^{-5} m/s, it can be observed that the thermal interaction effects between the two different PCMs (Case 3) can not be neglected. In the charging mode, the solid-liquid interface of the two different PCMs (Case 3) is almost the same compared with that presented in cases (1) and (2). The liquid fraction of PCM1 is increased from 0.46 to 0.47 and the latent heat energy stored is increased from 0.7728×10^5 to 0.7896×10^5 kJ/kg. However, the liquid fraction of PCM2 is decreased from 0.25 to 0.24 and the latent heat energy stored is decreased from 0.5×10^5 to 0.48×10^5 kJ/kg. The latent heat energy stored is 1.5456×10^5, 10^5 and 1.2696×10^5 kJ/kg in cases (1), (2) and (3), respectively. For an inlet velocity of 10^{-6} m/s, the liquid fraction of PCM1 is increased from 0.35 to 0.37 and the latent heat energy stored is increased from 0.588×10^5 to 0.6216×10^5 kJ/kg. However, the liquid fraction of PCM2 is decreased from 0.17 to 0.15 and the latent heat energy stored is decreased from 0.34×10^5 to 0.3×10^5 kJ/kg. The latent heat energy stored is 1.176×10^5, 0.68×10^5 and 0.9216×10^5 kJ/kg in cases (1), (2) and (3), respectively.

ISSN 2356-5608

In the discharging mode, the thermal interaction appears clearly for an inlet velocity of 10^{-5} and 10^{-6} m/s. It can be seen that the thermal discharging of PCM2 was accelerated and the thermal discharging of PCM1 was reduced in Case 3. For 10^{-5} m/s, the liquid fraction of PCM1 is increased from 0.81 to 0.88 and the latent heat energy stored is increased from 1.3608×10^5 to 1.4784×10^5 kJ/kg. However, the liquid fraction of PCM2 is reduced from 0.25 to 0.18 and the latent heat energy stored is reduced from 0.5×10^5 to 0.36×10^5 kJ/kg. The latent heat energy stored is 2.7216×10^5, 10^5 and 1.8384×10^5 kJ/kg in cases (1), (2) and (3), respectively. For 10^{-6} m/s, the liquid fraction of PCM1 is increased from 0.7 to 0.9 and the latent heat energy stored is increased from 1.176×10^5 to 1.8×10^5 kJ/kg.

However, the liquid fraction of PCM2 is reduced from 0.17 to 0.06 and the latent heat energy stored is reduced from 0.34×10^5 to 0.12×10^5 kJ/kg. The latent heat energy stored is 2.352×10^5, 0.68×10^5 and 1.92×10^5 kJ/kg in cases (1), (2) and (3), respectively.

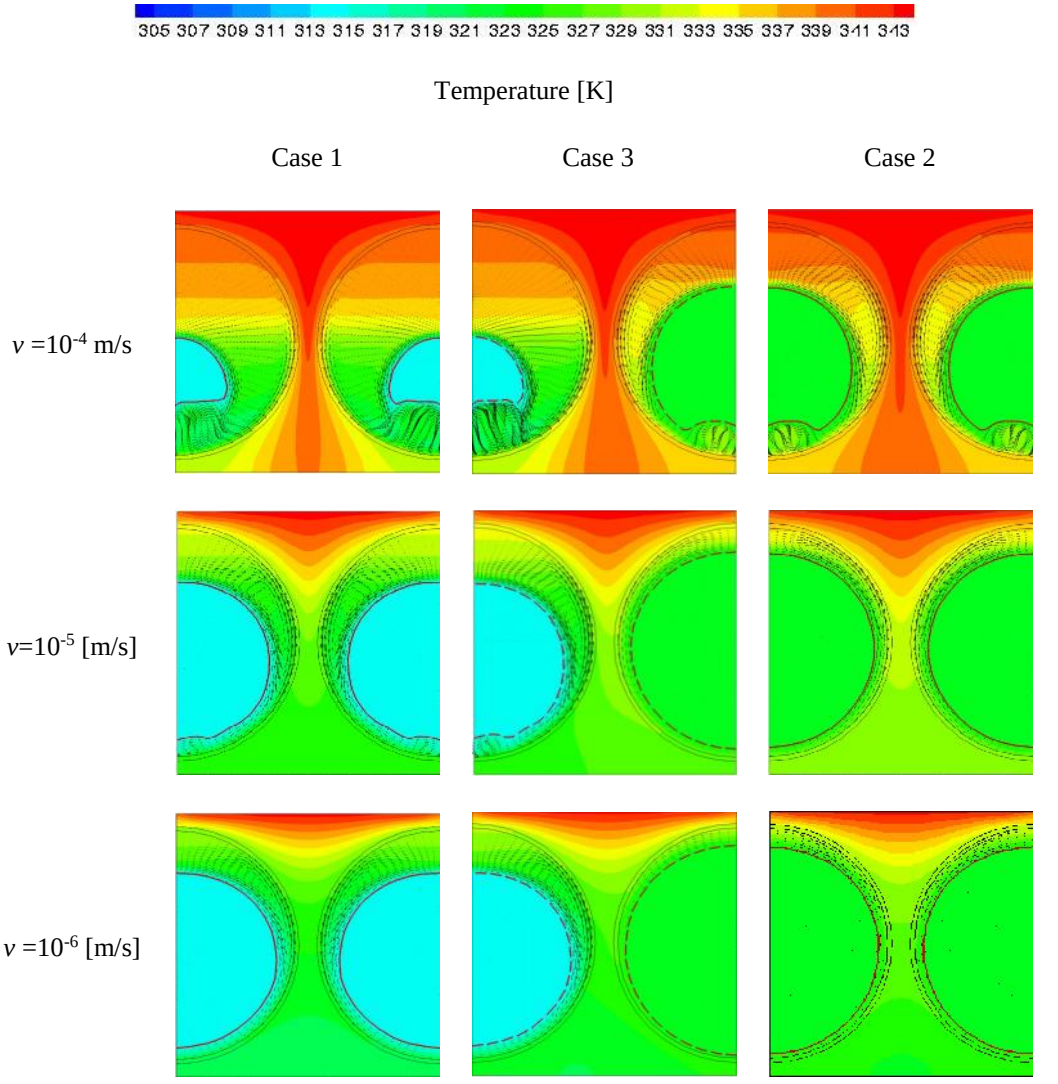

Fig.2 Velocity effect of water flow on the thermal behavior of two adjacent spheres filled with two different PCM (case 3) at t=2000 s, during charging mode.

ISSN 2356-5608

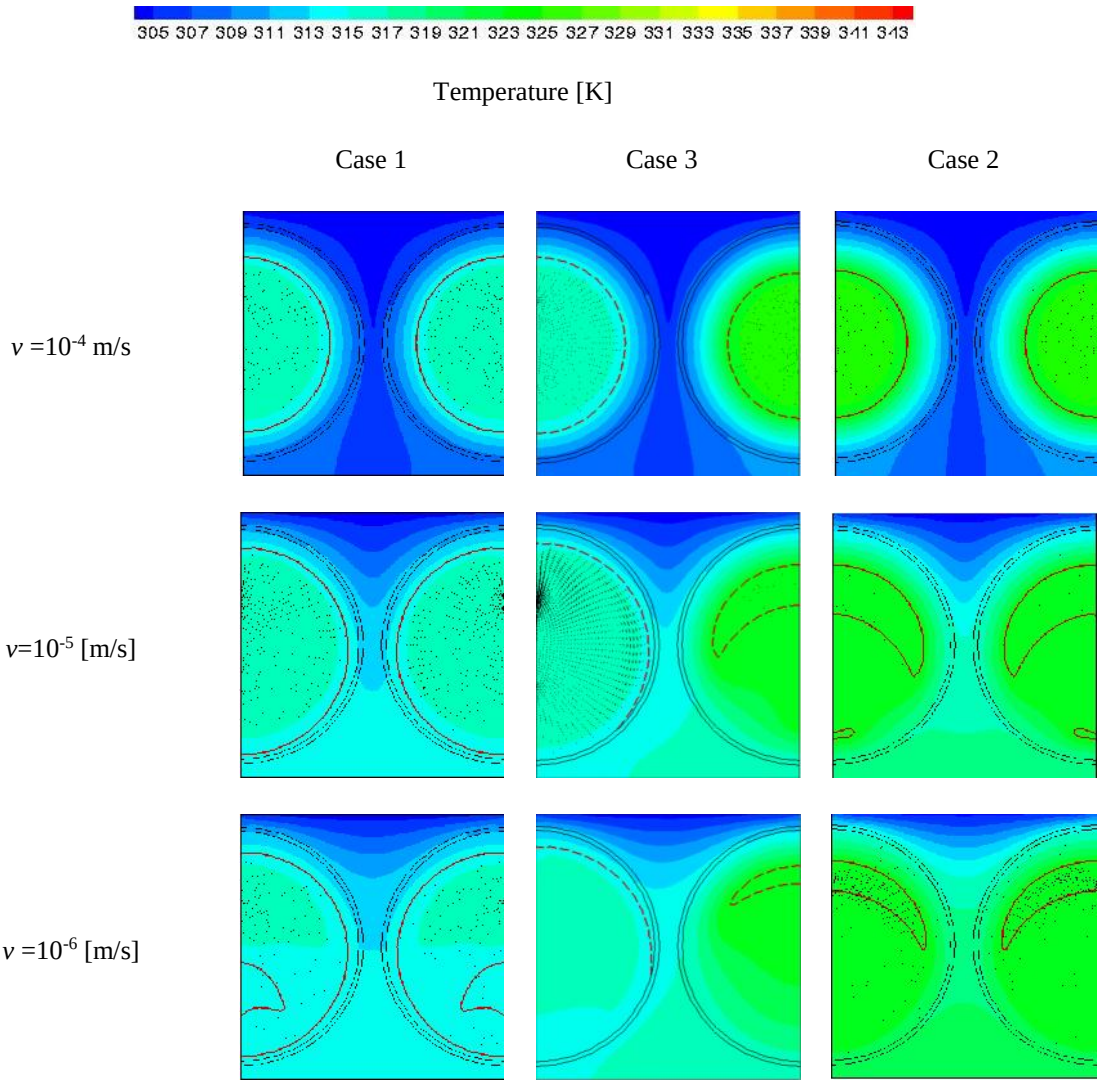

Fig.3 Velocity effect of water flow on the thermal behavior of two adjacent spheres filled with two different PCM ((case 3) PCM1-PCM2) at *t*=6000 *s* during discharging mode.

Table 2 latent heat energy stored [kJ/kg] by sphere in different cases during charging (at *t*=2000 s) and discharging (at *t*=6000 *s*) modes, with different flow velocity.

Charging mode at $t = 2000\ s$								
	Case 1		Case 3				Case 2	
Inlet velocity [m/s]	f_l PCM1	latent heat stored	f_l		latent heat stored		f_l PCM2	latent heat stored
			PCM1	PCM2	PCM1	PCM2		
10^{-4} m/s	0.87	1.4616×10^5	0.87	0.54	1.4616×10^5	1.08×10^5	0.54	1.08×10^5
10^{-5} m/s	0.46	0.7728×10^5	0.47	0.24	0.7896×10^5	0.48×10^5	0.25	0.5×10^5
10^{-6} m/s	0.35	0.588×10^5	0.37	0.15	0.6216×10^5	0.3×10^5	0.17	0.34×10^5

ISSN 2356-5608

Discharging mode at $t = 6000\ s$								
10^{-4} m/s	0.57	0.9576×10^{5}	0.57	0.39	0.9576×10^{5}	0.78×10^{5}	0.39	0.78×10^{5}
10^{-5} m/s	0.81	1.3608×10^{5}	0.88	0.18	1.4784×10^{5}	0.36×10^{5}	0.25	0.5×10^{5}
10^{-6} m/s	0.7	1.176×10^{5}	0.9	0.06	1.8×10^{5}	0.12×10^{5}	0.17	0.34×10^{5}

VI CONCLUSION

Numerical simulation of the thermal behavior of melting and solidification of two different PCMs, inside an aluminum sphere, was investigated in this paper. Stationary liquid water, at 70 ^{0}C in the charging mode and 32 ^{0}C during both charging and discharging mode. We can be conclude, that during the charging mode, increasing the inlet velocity from 10^{-5} to 10^{-4} m/s can increase the latent heat energy stored by 50%. This improvement becomes 27.41% when increasing the inlet velocity from 10^{-6} to 10^{-5} m/s. Moreover, during the discharging mode, increasing the inlet velocity form 10^{-5} to 10^{-4} m/s can decrease the latent heat energy stored by 5.48%. This reduction becomes 4.25% when increasing the inlet velocity form 10^{-6} to 10^{-5} m/s. Thus, with thermal interaction, the latent heat energy stored by two different PCMs (Case 3) is not the arithmetical addition of that stored with the same PCM in cases (1) and (2). Therefore, decreasing the velocity of the heat transfer fluid (water) increases the heat storage and accelerates the discharging mode.

REFERENCES

[1] M. Telkes, E. Raymond, Storing solar heat in chemicals-a report on the Dover house, Heat Vent. 46 (11) (1949) 80-86.

[2] H.G. Barkmann, F.C. Wessling, Use of buildings structural components for thermal storage, in: Proceedings of the Workshop on Solar Energy Storage Subsystems for the Heating and Cooling of Buildings. Charlottesville, Virginia, USA, 1975.

[3] D.W. Hawes, D. Feldman, D. Banu, Latent heat storage in building materials, Energy Build. 20 (1993) 77-86.

[4] C.H. Lee, H.K. Choi, Crystalline morphology in high-density polyethylene/ paraffin blend for thermal energy storage, Polym. Compos. 19 (6) (1998) 704-708.

[5] M. Sokolov, Y. Keizman, Performance indicators for solar pipes with phase change storage, Sol. Energy 47 (1991) 339-346.

[6] Y. Rabin, I. Bar-Niv, E. Korin, B. Mikic, Integrated solar collector storage system based on a salt-hydrate phase change material, Sol. Energy 55 (1995) 435-444.

[7] S.O. Enibe, Parametric effects on the performance of a passive solar air heater with storage, in: Proceedings of the World Renewable Energy Congress WII (2002) Cologne, Germany.

[8] S.O. Enibe, Performance of a natural circulation air heating system with phase change material energy storage, Renew. Energ. 27 (2002) 69-86.

[9] J. Tey, R. Fernandez, J. Rosell, M. Ibanez, Solar collector with integrated storage and transparent insulation cover, in: Proceedings of Eurosun. Bologna, Italy, 2002.

[10] F. Agyenim, N. Hewitt, P. Eames, M. Smyth, A review of materials, heat transfer and phase change problem formulation for latent heat thermal energy storage systems (LHTESS), Renew. Sust. Energ. Rev. 14 (2010) 615-628.

[11] M.M. Farid, A.M. Khudhair, S.A.K. Razack, S. Al-Hallaj, A review on phase change energy storage: materials and applications, Energ. Convers. Manage. 45 (2004) 1597-1615.

[12] B. Zalba, J.M. Marın, L.F. Cabeza, H. Mehling, Review on thermal energy storage with phase change: materials, heat transfer analysis and applications, Appl. Therm. Eng. 23 (2003) 251-283.

[13] Lacroix M. Modelling of latent heat storage systems. In: Dincer I, Rosen MA, editors. Thermal energy storage systems and applications. UK: Wiley; 2002.

[14] Korti, A. N.,Numerical Heat Flux Simulations on Double-Pass Solar Collector with PCM Spheres Media, International Journal of Air-Conditioning and Refrigeration,Vol. 24, No. 2 1650010 (13 pages),DOI: 10.1142/S2010132516500103 2016,(2016)

[15] Watanabe, T., Kikuchi, H. and Kanzawa, A., Enhancement of charging and discharging rates in a latent heat storage system by use of PCM with different melting temperatures, Heat Recovery Systems and CHP, Vol. 13 No. 1, pp. 57–66, (1993).

[16] Korti, A. N., Numerical simulation of fluid flow and heat transfer during the initial phase leading to steady state solidification in D. C. cast aluminum alloys, International Journal of Computational Methods, Vol. 7, No. 2, pp. 349-367. DOI No: 10.1142/S0219876210002222. ISSN: 0219-8762, (2010).

[17] Katsman, L., Investigation of phase change in cylindrical geometry with internal fins, M.Sc. Thesis, Heat Transfer Laboratory, Department of Mechanical Engineering, Ben-Gurion University of the Negev, Beer-Sheva, Israel, (2006).

ISSN 2356-5608